ELSEVIER

Comput. Methods Appl. Mech. Engrg. 147 (1997) 263–273

Computer methods in applied mechanics and engineering

Artificial boundary conditions for two-dimensional incompressible viscous flows around an obstacle

Weizhu Bao*

Department of Applied Mathematics, Tsinghua University, Beijing 100084, China

Received 30 July 1996; revised 14 November 1996

Abstract

In this paper we consider numerical simulation of incompressible viscous flow around an obstacle in velocity–pressure formulation. Two horizontal straight line artificial boundaries are introduced and the original flow is approximated by a flow in an infinite channel with slip boundary condition on the wall. Then two vertical segment artificial boundaries are introduced to limit the channel to a bounded computational domain. In the region of the channel between the vertical boundaries and infinity, the velocity of the flow is almost a constant vector, in which the Navier–Stokes equations can be linearised by Oseen equations and thus a general solution can be derived by using separation of variables. Artificial boundary conditions on the vertical segments are then designed by imposing the continuity of velocity and normal stress. Therefore, the original problem is reduced to a boundary value problem on a bounded computational domain. Numerical example shows that our artificial boundary conditions are very effective.

1. Introduction

Let Ω_i be a bounded domain in $\mathbb{R}^2$, with a simple closed curve boundary. Consider the Navier–Stokes equations in the exterior domain $\mathbb{R}^2 \setminus \bar{\Omega}_i$, under Dirichlet boundary conditions:

$$(u \cdot \nabla)u + \nabla p = \nu\, \Delta u, \quad \text{in } \mathbb{R}^2 \setminus \bar{\Omega}_i, \tag{1.1}$$

$$\nabla \cdot u = 0, \quad \text{in } \mathbb{R}^2 \setminus \bar{\Omega}_i, \tag{1.2}$$

$$u|_{\partial\Omega_i} = 0, \tag{1.3}$$

$$u(x) \to u_\infty \equiv (a, 0)^{\mathrm{T}}, \quad \text{when } r = \sqrt{x_1^2 + x_2^2} \to \infty, \tag{1.4}$$

where $u = (u_1, u_2)^{\mathrm{T}}$ is the velocity, p is the pressure, $\nu > 0$ is the viscosity coefficient, $a > 0$ is a constant, $x = (x_1, x_2)^{\mathrm{T}}$.

The boundary value problem (1.1)–(1.4) describes motion of a viscous, incompressible fluid flow around an obstacle of shape Ω_i, with no movement of the fluid particles on the boundary of Ω_i. In finding numerical solutions of this kind of problem defined in unbounded domain, one difficulty is the unboundedness of the physical domain. In engineering, the usual method is to introduce an artificial boundary and cut off the unbounded part of the domain and to set up an artificial boundary condition at the artificial boundary of the remaining bounded domain. For example, the Dirichlet condition and

*Current address: Imperial College, Department of Mathematics, 180 Queen's Gate, London SW7 2BZ, UK.

0045-7825/97/$17.00
PII S0045-7825(97)00001-7

Neumann condition are often used for elliptic partial differential equations. In general, this artificial boundary condition at the artificial boundary is only a rough approximation of the exact boundary condition. Hence, the remaining bounded domain must be quite large when high accuracy is required. In practice, in order to limit the computational cost, the artificial boundary must be chosen not too far from the domain of interest. During the last ten years, ways to design artificial boundary conditions with high accuracy on a given artificial boundary for solving N–S equations in an unbounded domain have been studied often. For instance, Halpern [1], Halpern and Schatzman [2] designed a family of artificial boundary conditions for unsteady Oseen equations in the velocity pressure formulation and applied them to solve unsteady N–S equations. Nataf [3] presented an open boundary condition for steady Oseen equations in stream-function vorticity formulation, which is applied to viscous incompressible flow around a body in a flat channel with slip boundary conditions on the wall. Hagstrom [4,5] proposed asymptotic boundary conditions at artificial boundaries for the simulation of time-dependent fluid flow and applied them to solve N–S equations. Han et al. [6], Han and Bao [7,8] developed artificial boundary conditions for N–S equations with stream-function vorticity formulation in channel.

In this paper we consider a steady viscous incompressible flow around an obstacle with velocity–pressure formulation. Two horizontal straight line artificial boundaries are introduced and the problem (1.1)–(1.4) is approximated by a flow in an infinite channel with slip boundary condition on the wall. Then, two vertical segments are introduced to limit the channel to a bounded computational domain. In the region sufficiently far from the obstacle, the velocity of the flow is almost a constant vector, in which N–S equations can be linearised by Oseen equations. A series of artificial boundary conditions with increasing accuracy are designed by imposing the continuity of velocity and the normal stress. Thus, the original problem (1.1)–(1.4) is approximated by a problem defined in a bounded computational domain. Numerical results show that our artificial boundary conditions are very effective.

2. The exterior Navier–Stokes problem

Taking a constant $L > 0$, such that $\bar{\Omega}_i \subset \Omega \equiv \mathbb{R} \times (0, L)$, then the exterior Navier–Stokes problem (1.1)–(1.4) is approximated by the following problem when L is sufficiently large [3]:

$$(u \cdot \nabla)u + \nabla p = \nu \, \Delta u, \quad \text{in } \Omega \backslash \bar{\Omega}_i, \tag{2.1}$$

$$\nabla \cdot u = 0, \quad \text{in } \Omega \backslash \bar{\Omega}_i, \tag{2.2}$$

$$u_2|_{x_2=0,L} = 0, \qquad \sigma_{12}|_{x_2=0,L} \equiv \nu \left(\frac{\partial u_1}{\partial x_2} + \frac{\partial u_2}{\partial x_1} \right) \bigg|_{x_2=0,L} = 0, \quad -\infty < x_1 < +\infty, \tag{2.3}$$

$$u|_{\partial \Omega_i} = 0, \tag{2.4}$$

$$u(x) \to u_\infty, \quad \text{when } x_1 \to \pm\infty, \tag{2.5}$$

where σ_{12} is the tangential stress on the wall. The boundary condition (2.3) is called slip boundary condition and is equivalent to the following:

$$\frac{\partial u_1}{\partial x_2} \bigg|_{x_2=0,L} = u_2|_{x_2=0,L} = 0, \quad -\infty < x_1 < +\infty, \tag{2.6}$$

Taking two constants $b < c$, such that $\Omega_i \subset (b, c) \times (0, L)$, then Ω is divided into three parts Ω_b, Ω_T and Ω_c by the artificial boundaries Γ_b and Γ_c with

$$\Gamma_b = \{x \in \mathbb{R}^2 \mid x_1 = b, \, 0 \leqslant x_2 \leqslant L\},$$
$$\Gamma_c = \{x \in \mathbb{R}^2 \mid x_1 = c, \, 0 \leqslant x_2 \leqslant L\},$$
$$\Omega_b = \{x \in \mathbb{R}^2 \mid -\infty < x_1 < b, \, 0 < x_2 < L\},$$
$$\Omega_T = \{x \in \mathbb{R}^2 \mid b < x_1 < c, \, 0 < x_2 < L\} \setminus \bar{\Omega}_i,$$
$$\Omega_c = \{x \in \mathbb{R}^2 \mid c < x_1 < +\infty, \, 0 < x_2 < L\}.$$

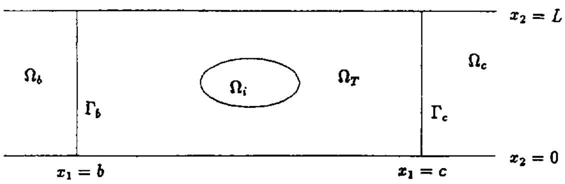

Fig. 1.

When $|b|$ and c are sufficiently large, in the domain $\Omega_b \cup \Omega_c$ the velocity u is almost constant vector u_∞. So the N–S equations (2.1)–(2.2) can be linearised in domain Ω_c (and Ω_b), namely the solution (u,p) of problem (2.1)–(2.5) approximately satisfies the following problem [2,6–8]:

$$a\frac{\partial u}{\partial x_1} + \nabla p = \nu\,\Delta u, \quad \text{in } \Omega_c, \tag{2.7}$$

$$\nabla \cdot u = 0, \quad \text{in } \Omega_c, \tag{2.8}$$

$$\left.\frac{\partial u_1}{\partial x_2}\right|_{x_2=0,L} = u_2|_{x_2=0,L} = 0, \quad c \leqslant x_1 < +\infty, \tag{2.9}$$

$$u(x) \to u_\infty, \quad \text{when } x_1 \to +\infty. \tag{2.10}$$

In [9], the author derived a general solution of the above problem using separation of variables under the assumption $\lim_{x_1\to\infty} p(x) = p_\infty = 0$:

$$u_1(x) = a + \sum_{m=1}^{\infty}\left[a_m\,\mathrm{e}^{-\frac{m\pi}{L}(x_1-c)} - \frac{m\pi}{L\lambda^-(m)}\,b_m\,\mathrm{e}^{\lambda^-(m)(x_1-c)}\right]\cos\frac{m\pi x_2}{L}, \tag{2.11}$$

$$u_2(x) = \sum_{m=1}^{\infty}\left[a_m\,\mathrm{e}^{-\frac{m\pi}{L}(x_1-c)} + b_m\,\mathrm{e}^{\lambda^-(m)(x_1-c)}\right]\sin\frac{m\pi x_2}{L}, \tag{2.12}$$

$$p(x) = -a\sum_{m=1}^{\infty} a_m\,\mathrm{e}^{-\frac{m\pi}{L}(x_1-c)}\cos\frac{m\pi x_2}{L}, \tag{2.13}$$

where

$$\lambda^-(m) = \frac{a - \sqrt{a^2 + 4\nu^2 m^2\pi^2/L^2}}{2\nu}, \quad m = 1,2,\ldots,$$

$a_1,\ b_1,\ a_2,\ b_2,\ \ldots$ are any constants.

3. Artificial boundary conditions on Γ_c

Let $\varepsilon(u) = (\varepsilon_{ij}(u))_{2\times2}$ and $\sigma(u,p) = (\sigma_{ij}(u,p))_{2\times2}$ denote the rate of strain and stress tensors, respectively. We have

$$\varepsilon_{ij}(u) = \frac{1}{2}\left(\frac{\partial u_i}{\partial x_j} + \frac{\partial u_j}{\partial x_i}\right), \quad i,j = 1,2 \tag{3.1}$$

and

$$\sigma_{ij}(u,p) = -p\delta_{ij} + 2\nu\,\varepsilon_{ij}(u), \quad i,j = 1,2, \tag{3.2}$$

where δ_{ij} is the Kronecker Delta whose properties are

$$\delta_{ij} = \begin{cases} 1, & i = j, \\ 0, & i \neq j. \end{cases}$$

$\sigma_n = (\sigma_{n_1}, \sigma_{n_2})^{\mathrm{T}}$ denotes the normal stress on the artificial boundary Γ_c, then

$$\sigma_{n_1} = n_1\sigma_{11} + n_2\sigma_{12} = \sigma_{11} = \left(-p + 2\nu \frac{\partial u_1}{\partial x_1}\right)\bigg|_{\Gamma_c}, \tag{3.3}$$

$$\sigma_{n_2} = n_1\sigma_{21} + n_2\sigma_{22} = \sigma_{21} = \nu\left(\frac{\partial u_1}{\partial x_2} + \frac{\partial u_2}{\partial x_1}\right)\bigg|_{\Gamma_c}, \tag{3.4}$$

where $n = (n_1, n_2)^{\mathrm{T}} = (1, 0)^{\mathrm{T}}$ is the outward normal vector on Γ_c.

We now use the transmission conditions

$$u(c^-, x_2) = u(c^+, x_2), \tag{3.5}$$

$$\sigma_n(c^-, x_2) = \sigma_n(c^+, x_2), \tag{3.6}$$

to obtain artificial boundary conditions on the segment Γ_c for the problem (2.1)–(2.5). Substituting (2.11)–(2.13) into (3.3)–(3.4), we get

$$\sigma_{n_1} = \sum_{m=1}^{\infty}\left[\left(a - \frac{2\nu m\pi}{L}\right)a_m - \frac{2\nu m\pi}{L} b_m\right] \cos\frac{m\pi x_2}{L}, \tag{3.7}$$

$$\sigma_{n_2} = \nu\sum_{m=1}^{\infty}\left[-\frac{2m\pi}{L} a_m + \left(\lambda^-(m) + \frac{m^2\pi^2}{L^2\lambda^-(m)}\right) b_m\right] \sin\frac{m\pi x_2}{L}. \tag{3.8}$$

From (2.11)–(2.12) and (3.7)–(3.8), a computation shows

$$\begin{aligned} \sigma_{n_1} = \sum_{m=1}^{\infty}\bigg[& \frac{2\nu(-m\pi + L\lambda^-(m))}{L^2}\int_0^L u_1(c, x_2)\cos\frac{m\pi x_2}{L}\,\mathrm{d}x_2 \\ & - \frac{2\nu m\pi(m\pi + L\lambda^-(m))}{L^3\lambda^-(m)}\int_0^L u_2(c, x_2)\sin\frac{m\pi x_2}{L}\,\mathrm{d}x_2\bigg] \cos\frac{m\pi x_2}{L} \equiv T_1(u), \end{aligned} \tag{3.9}$$

$$\begin{aligned} \sigma_{n_2} = \sum_{m=1}^{\infty}\bigg[& \frac{-2\nu(m\pi + L\lambda^-(m))}{L^2}\int_0^L u_1(c, x_2)\cos\frac{m\pi x_2}{L}\,\mathrm{d}x_2 \\ & + \frac{2\nu(-m\pi + L\lambda^-(m))}{L^2}\int_0^L u_2(c, x_2)\sin\frac{m\pi x_2}{L}\,\mathrm{d}x_2\bigg] \sin\frac{m\pi x_2}{L} \equiv T_2(u). \end{aligned} \tag{3.10}$$

Therefore, we obtain artificial boundary condition (3.9)–(3.10) on the artificial boundary Γ_c. Let

$$T(u) = \begin{pmatrix} T_1(u) \\ T_2(u) \end{pmatrix}.$$

Then, the problem (2.1)–(2.5) ($\equiv$ (1.1)–(1.4)) can be reduced to the following problem in a bounded computational domain Ω_T:

$$(u \cdot \nabla)u + \nabla p = \nu\,\Delta u, \quad \text{in } \Omega_T, \tag{3.11}$$

$$\nabla \cdot u = 0, \quad \text{in } \Omega_T, \tag{3.12}$$

$$\left.\frac{\partial u_1}{\partial x_2}\right|_{x_2=0,L} = u_2|_{x_2=0,L} = 0, \quad b \leqslant x_1 \leqslant c, \tag{3.13}$$

$$u|_{\partial\Omega_i} = 0, \tag{3.14}$$

$$u|_{\Gamma_b} = u_\infty, \tag{3.15}$$

$$\sigma_n = T(u), \quad \text{on } \Gamma_c. \tag{3.16}$$

Let

$$T_1^N(u) = \sum_{m=1}^{N}\left[\frac{2\nu(-m\pi + L\lambda^-(m))}{L^2}\int_0^L u_1(c,x_2)\cos\frac{m\pi x_2}{L}\,\mathrm{d}x_2 - \frac{2\nu m\pi(m\pi + L\lambda^-(m))}{L^3\lambda^-(m)}\int_0^L u_2(c,x_2)\sin\frac{m\pi x_2}{L}\,\mathrm{d}x_2\right]\cos\frac{m\pi x_2}{L}, \tag{3.17}$$

$$T_2^N(u) = \sum_{m=1}^{N}\left[\frac{-2\nu(m\pi + L\lambda^-(m))}{L^2}\int_0^L u_1(c,x_2)\cos\frac{m\pi x_2}{L}\,\mathrm{d}x_2 + \frac{2\nu(-m\pi + L\lambda^-(m))}{L^2}\int_0^L u_2(c,x_2)\sin\frac{m\pi x_2}{L}\,\mathrm{d}x_2\right]\sin\frac{m\pi x_2}{L}, \tag{3.18}$$

$$T^N(u) = \begin{pmatrix} T_1^N(u) \\ T_2^N(u) \end{pmatrix}.$$

Then, we get a sequence of approximate artificial boundary conditions on the segment Γ_c.

$$\sigma_n = T^N(u), \quad N = 0,1,2,\ldots, \tag{3.19}$$

where

$$T^0(u) = \begin{pmatrix} 0 \\ 0 \end{pmatrix}.$$

Hence, the original problem (1.1)–(1.4) is reduced to the following problem in the bounded computational domain Ω_T approximately for $N = 0,1,2,\ldots$

$$(u\cdot\nabla)u + \nabla p = \nu\,\Delta u, \quad \text{in } \Omega_T, \tag{3.20}$$

$$\nabla\cdot u = 0, \quad \text{in } \Omega_T, \tag{3.21}$$

$$\left.\frac{\partial u_1}{\partial x_2}\right|_{x_2=0,L} = u_2|_{x_2=0,L} = 0, \quad b \leqslant x_1 \leqslant c, \tag{3.22}$$

$$u|_{\partial\Omega_i} = 0, \tag{3.23}$$

$$u|_{\Gamma_b} = u_\infty, \tag{3.24}$$

$$\sigma_n = T^N(u), \quad \text{on } \Gamma_c. \tag{3.25}$$

In fact, $N = 0$ in (3.19) is the stress-free boundary condition which is often used in engineering to solve N–S equations.

In a similar way, we can derive approximate artificial boundary conditions on the artificial boundary Γ_b.

4. The finite element solutions of problems (3.11)–(3.16) and (3.20)–(3.25)

Let $H^m(\Omega_T)$ denote the usual Sobolev spaces on the domain Ω_T with integer m [10]. Furthermore, let

$$\Gamma_1 = \{x \in \mathbb{R}^2 \mid x_2 = 0,\ b \leqslant x_1 \leqslant c\} \cup \{x \in \mathbb{R}^2 \mid x_2 = L,\ b \leqslant x_1 \leqslant c\},$$
$$\Gamma_i = \partial\Omega_i,$$
$$V = \{v \in H^1(\Omega_T) \times H^1(\Omega_T) \mid v|_{\Gamma_b \cup \Gamma_i} = 0,\ v_2|_{\Gamma_1} = 0\},$$

with norm $\|v\|_V^2 = \|v_1\|_{1,2,\Omega_T}^2 + \|v_2\|_{1,2,\Omega_T}^2$,

$$W = L^2(\Omega_T) \quad \text{with norm } \|q\|_W = \|q\|_{L^2(\Omega_T)},$$
$$M = \{v \in H^1(\Omega_T) \times H^1(\Omega_T) \,|\, v|_{\Gamma_i} = 0,\ v|_{\Gamma_b} = u_\infty,\ v_2|_{\Gamma_1} = 0\}.$$

Then, the boundary value problem (3.11)–(3.16) is equivalent to the following variational problem:

Find $(u,p) \in M \times W$, such that

$$A(u,v) + A_0(u,u,v) + A_1(u,v) + B(v,p) = 0, \quad \forall v \in V, \tag{4.1}$$
$$B(u,q) = 0, \quad \forall q \in W, \tag{4.2}$$

where

$$A(u,v) = 2\nu \int_{\Omega_T} \sum_{i,j=1}^{2} \varepsilon_{ij}(u) \cdot \varepsilon_{ij}(v)\,\mathrm{d}x \equiv 2\nu \int_{\Omega_T} \varepsilon(u) \cdot \varepsilon(v)\,\mathrm{d}x,$$

$$A_0(u,v,w) = \int_{\Omega_T} [(u \cdot \nabla)v] \cdot w\,\mathrm{d}x = \int_{\Omega_T} \sum_{i,j=1}^{2} u_i \frac{\partial v_j}{\partial x_i} w_j\,\mathrm{d}x,$$

$$B(u,q) = -\int_{\Omega_T} q\nabla \cdot u\,\mathrm{d}x.$$

$$\begin{aligned} A_1(u,v) &= -\int_{\Gamma_c} \sigma_n \cdot v\,\mathrm{d}x_2 \\ &= -\int_{\Gamma_c} T(u) \cdot v\,\mathrm{d}x_2 \\ &= \sum_{m=1}^{\infty} \Bigg[\frac{2\nu(m\pi - L\lambda^-(m))}{L^2} \int_0^L u_1(c,x_2) \cos\frac{m\pi x_2}{L}\,\mathrm{d}x_2 \int_0^L v_1(c,x_2)\cos\frac{m\pi x_2}{L}\,\mathrm{d}x_2 \\ &\quad + \frac{2\nu m\pi(m\pi + L\lambda^-(m))}{L^3\lambda^-(m)} \int_0^L u_2(c,x_2)\sin\frac{m\pi x_2}{L}\,\mathrm{d}x_2 \int_0^L v_1(c,x_2)\cos\frac{m\pi x_2}{L}\,\mathrm{d}x_2 \\ &\quad + \frac{2\nu(m\pi + L\lambda^-(m))}{L^2} \int_0^L u_1(c,x_2)\cos\frac{m\pi x_2}{L}\,\mathrm{d}x_2 \int_0^L v_2(c,x_2)\sin\frac{m\pi x_2}{L}\,\mathrm{d}x_2 \\ &\quad + \frac{2\nu(m\pi - L\lambda^-(m))}{L^2} \int_0^L u_2(c,x_2)\sin\frac{m\pi x_2}{L}\,\mathrm{d}x_2 \int_0^L v_2(c,x_2)\sin\frac{m\pi x_2}{L}\,\mathrm{d}x_2 \Bigg]. \end{aligned}$$

Furthermore, let

$$
\begin{aligned}
A_1^N(u,v) &= -\int_{\Gamma_c} T^N(u)\cdot v\,\mathrm{d}x_2 \\
&= \sum_{m=1}^{N}\Bigg[\frac{2\nu(m\pi - L\lambda^-(m))}{L^2}\int_0^L u_1(c,x_2)\cos\frac{m\pi x_2}{L}\,\mathrm{d}x_2\int_0^L v_1(c,x_2)\cos\frac{m\pi x_2}{L}\,\mathrm{d}x_2 \\
&\quad+\frac{2\nu m\pi(m\pi + L\lambda^-(m))}{L^3\lambda^-(m)}\int_0^L u_2(c,x_2)\sin\frac{m\pi x_2}{L}\,\mathrm{d}x_2\int_0^L v_1(c,x_2)\cos\frac{m\pi x_2}{L}\,\mathrm{d}x_2 \\
&\quad+\frac{2\nu(m\pi + L\lambda^-(m))}{L^2}\int_0^L u_1(c,x_2)\cos\frac{m\pi x_2}{L}\,\mathrm{d}x_2\int_0^L v_2(c,x_2)\sin\frac{m\pi x_2}{L}\,\mathrm{d}x_2 \\
&\quad+\frac{2\nu(m\pi - L\lambda^-(m))}{L^2}\int_0^L u_2(c,x_2)\sin\frac{m\pi x_2}{L}\,\mathrm{d}x_2\int_0^L v_2(c,x_2)\sin\frac{m\pi x_2}{L}\,\mathrm{d}x_2\Bigg].
\end{aligned}
$$

Then, the boundary value problem (3.20)–(3.25) is equivalent to the following variational problem:

Find $(u_N, p_N) \in M \times W$, such that

$$A(u_N, v) + A_0(u_N, u_N, v) + A_1^N(u_N, v) + B(v, p_N) = 0, \quad \forall v \in V, \tag{4.3}$$

$$B(u_N, q) = 0, \quad \forall q \in W. \tag{4.4}$$

Let $\mathcal{T}_h$ be a regular partition of the domain Ω_T, suppose V_h and W_h are finite element subspaces of V and W. Particularly, we also assume they are the optimally compatible. Then V_h and W_h should satisfy the following conditions [11].

(a) The errors $\inf_{v\in V_h}\|u-v\|_V$ and $\inf_{q\in W_h}\|p-q\|_W$ have the same order in h, i.e. there is a constant α, such that

$$\inf_{v\in V_h}\|u-v\|_V \leqslant \alpha h^m |u|_{m+1,2,\Omega_T}, \qquad \inf_{q\in W_h}\|p-q\|_W \leqslant \alpha h^m |p|_{m,2,\Omega_T}. \tag{4.5}$$

(b) There exists a constant β independent of h, such that

$$\sup_{v\in V_h\setminus\{0\}} \frac{B(v,q)}{\|v\|_V} \geqslant \beta\|q\|_W, \quad \forall q \in W_h. \tag{4.6}$$

Let M_h be a subset of M, which satisfies $V_h = \{u_h - v_h \mid \forall u_h, v_h \in M_h\}$. Then the finite element approximation of (4.3)–(4.4) is

Find $(u_N^h, p_N^h) \in M_h \times W_h$, such that

$$A(u_N^h, v) + A_0(u_N^h, u_N^h, v) + A_1^N(u_N^h, v) + B(v, p_N^h) = 0, \quad \forall v \in V_h, \tag{4.7}$$

$$B(u_N^h, q) = 0, \quad \forall q \in W_h. \tag{4.8}$$

5. Numerical implementation and example

For the sake of simplicity, Let $\mathcal{T}_h$ be a rectangle partition of Ω_T, with

$$\Omega_T = \bigcup_{K\in\mathcal{T}_h} K,$$

where K is a rectangle.

For each rectangle $K \in \mathcal{T}_h$, connect the mid-points of the opposite sides of K, then each rectangle K is divided into four smaller rectangles. Let $\mathcal{T}_{\hat{h}}$ denote this new partition. Let

$$
\begin{aligned}
V_h &= \{v \in V \mid v|_K \text{ is a bilinear polynomial}, \ \forall K \in \mathcal{T}_{\hat{h}}\}, \\
W_h &= \{p \in W \mid p|_K \text{ is constant}, \ \forall K \in \mathcal{T}_h\}, \\
M_h &= \{v \in M \mid v|_K \text{ is a bilinear polynomial}, \ \forall K \in \mathcal{T}_{\hat{h}}\}.
\end{aligned}
$$

Then V_h and W_h satisfy the Babuška–Brezzi (B–B) condition and the following approximation property [11]

$$\inf_{v \in V_h} \|u - v\|_V \leqslant Ch|u|_{2,2,\Omega_T},$$

$$\inf_{q \in W_h} \|p - q\|_V \leqslant Ch|p|_{1,2,\Omega_T}.$$

We use this finite element method to solve the following example.

EXAMPLE. Flow around a rectangular cylinder obstacle. The obstacle Ω_i is defined by the domain

$$\Omega_i = \left\{ x \in \mathbb{R}^2 \mid 0.8 < x_1 < 1.2,\ \frac{2L}{5} < x_2 < \frac{3L}{5} \right\}.$$

Then the bounded computational domain Ω_T is given by

$$\Omega_T = \{x \in \mathbb{R}^2 \mid b < x_1 < c,\ 0 < x_2 < L\} \setminus \bar{\Omega}_i.$$

We take $b = 0, c = 2.8, L = 1.0, a = 1.0$. The nonlinear term $(u \cdot \nabla)u$ is linearised by the Newton method. At every iterative step, we use the finite element method to solve a linear problem.

As Ω_i is a rectangular, we assume symmetry of the flow and consider only the upper half-domain of Ω_T. Thus, the following slip boundary condition is posed on the boundary $\Gamma = \{(x_1, L/2) \mid b \leqslant x_1 \leqslant 0.8$ or $1.2 \leqslant x_1 \leqslant c\}$:

$$\frac{\partial u_1(x)}{\partial x_2} = u_2(x) = 0, \quad x \in \Gamma. \tag{5.1}$$

Two meshes are used in the computation. Fig. 2 shows the partition $\mathcal{T}_h$ for mesh A of Ω_T. Mesh B is generated by dividing each rectangle in mesh A into four equal smaller rectangles. To test the effect of the approximate artificial boundary condition (3.19), let (u^h_∞, p^h_∞) denote the finite element solutions of the problem (4.7)–(4.8) with $N = N^*$ sufficiently large. In our computation we take $N^* = 100$. Let (u^h_N, p^h_N) denote the finite element solution of the problem (4.7)–(4.8).

Tables 1–6 show the maximum of the errors $u^h_\infty - u^h_N$ and $p^h_\infty - p^h_N$ over mesh points for mesh A and B with different kinematic viscosity ν. Furthermore, Fig. 3 shows the velocity field for mesh B with $\nu = 0.05$. Figs. 4 and 5 show the velocity for mesh B with $\nu = 0.05$. Figs. 6–11 show the errors $u^h_\infty - u^h_N$ and $p^h_\infty - p^h_N$ at outflow boundary Γ_c for meshes A and B with $\nu = 0.01$.

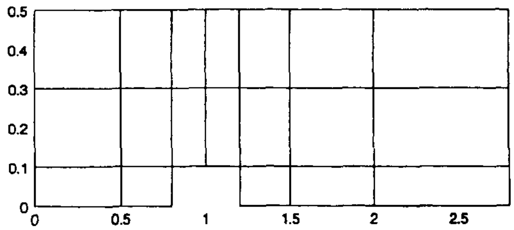

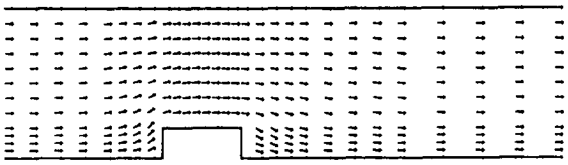

Fig. 2. Mesh A.

Fig. 3. Velocity field ($\nu = 0.05$).

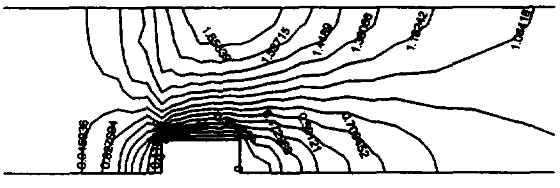

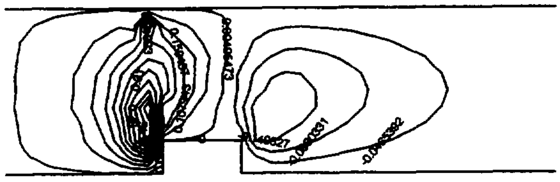

Fig. 4. u_1 ($\nu = 0.05$).

Fig. 5. u_2 ($\nu = 0.05$).

From Tables 1–6 and Figs. 6–11, we can see that the approximate artificial boundary condition (3.19) is very effective for the N–S equations and more accurate than the stress-free boundary condition which is often used in engineering literatures. Also, when N in (3.19) becomes larger, the artificial boundary condition (3.19) becomes more accuracy. The results also suggest that only a few terms in the bilinear form $A_1(u, v)$ are needed in order to get good accuracy.

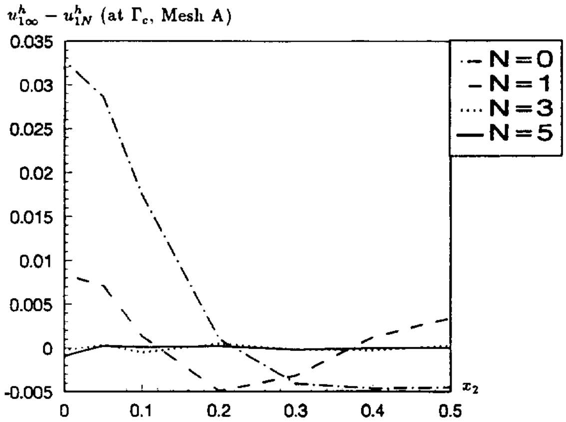

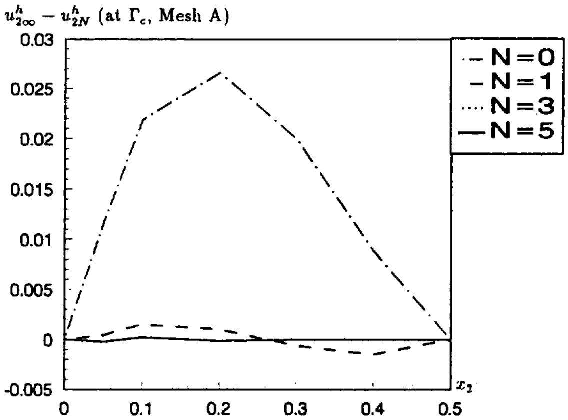

Fig. 6. $\nu = 0.01,\ c = 2.8$.
Fig. 7. $\nu = 0.01,\ c = 2.8$.

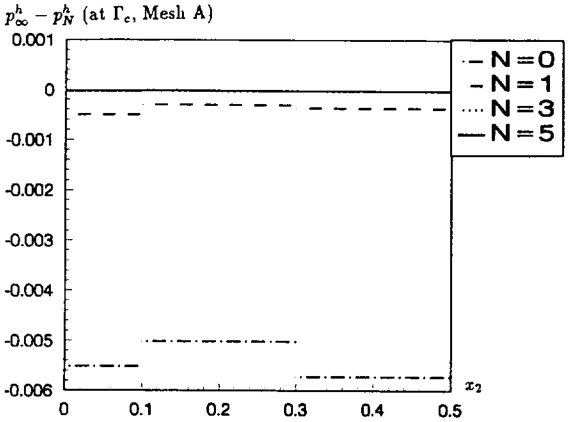

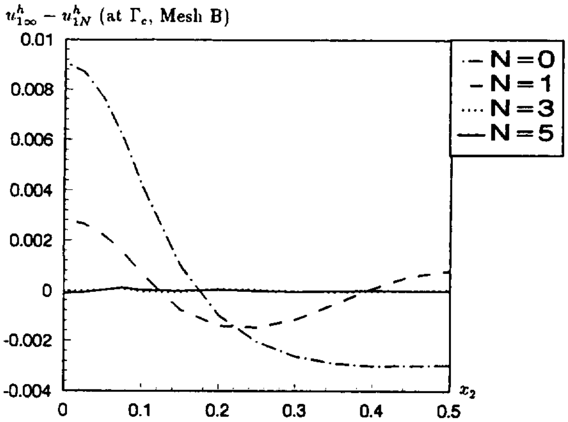

Fig. 8. $\nu = 0.01,\ c = 2.8$.
Fig. 9. $\nu = 0.01,\ c = 2.8$.

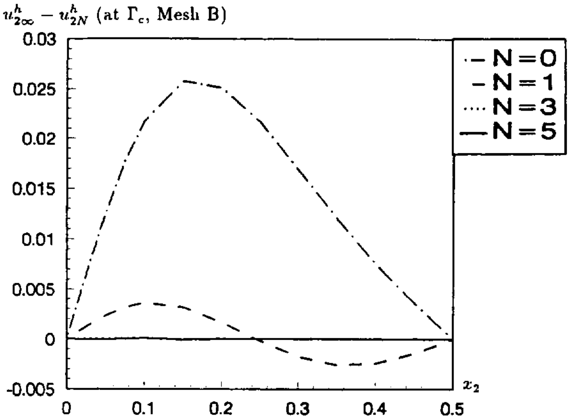

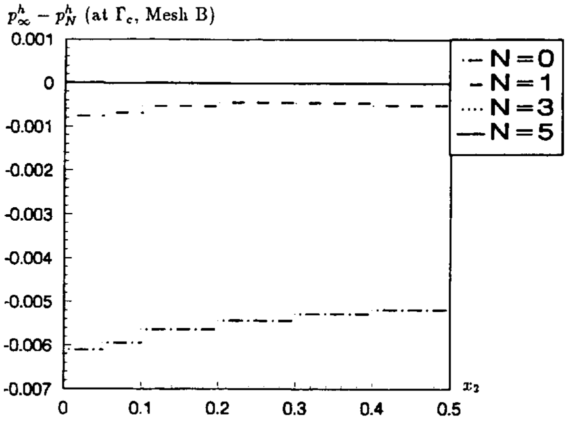

Fig. 10. $\nu = 0.01,\ c = 2.8$.
Fig. 11. $\nu = 0.01,\ c = 2.8$.

Table 1
$\nu = 0.05$, mesh A

N	$N = 0$	$N = 1$	$N = 3$	$N = 5$
$\max \lvert u^h_{1\infty} - u^h_{1N} \rvert$	1.267E-2	3.404E-4	2.137E-4	2.324E-4
$\max \lvert u^h_{2\infty} - u^h_{2N} \rvert$	1.195E-2	1.169E-3	4.605E-4	1.579E-4
$\max \lvert p^h_{\infty} - p^h_{N} \rvert$	4.297E-3	2.041E-4	4.197E-5	2.230E-5

Table 2
$\nu = 0.05$, mesh B

N	$N = 0$	$N = 1$	$N = 3$	$N = 5$
$\max \lvert u^h_{1\infty} - u^h_{1N} \rvert$	1.069E-2	7.668E-5	2.165E-5	2.664E-5
$\max \lvert u^h_{2\infty} - u^h_{2N} \rvert$	1.181E-2	5.725E-5	1.216E-5	6.459E-6
$\max \lvert p^h_{\infty} - p^h_{N} \rvert$	5.593E-3	3.171E-5	5.948E-6	7.687E-6

Table 3
$\nu = 0.02$, mesh A

N	$N = 0$	$N = 1$	$N = 3$	$N = 5$
$\max \lvert u^h_{1\infty} - u^h_{1N} \rvert$	2.898E-2	3.324E-3	4.403E-4	7.041E-4
$\max \lvert u^h_{2\infty} - u^h_{2N} \rvert$	2.810E-2	8.572E-4	3.690E-4	2.000E-4
$\max \lvert p^h_{\infty} - p^h_{N} \rvert$	7.881E-3	1.542E-4	3.362E-5	3.147E-5

Table 4
$\nu = 0.02$, mesh B

N	$N = 0$	$N = 1$	$N = 3$	$N = 5$
$\max \lvert u^h_{1\infty} - u^h_{1N} \rvert$	1.259E-2	5.754E-4	6.531E-5	9.108E-5
$\max \lvert u^h_{2\infty} - u^h_{2N} \rvert$	2.532E-2	5.679E-4	5.437E-5	3.767E-5
$\max \lvert p^h_{\infty} - p^h_{N} \rvert$	6.333E-3	1.155E-4	9.581E-6	1.343E-5

Table 5
$\nu = 0.01$, mesh A

N	$N = 0$	$N = 1$	$N = 3$	$N = 5$
$\max \lvert u^h_{1\infty} - u^h_{1N} \rvert$	3.271E-2	8.396E-3	5.245E-4	9.154E-4
$\max \lvert u^h_{2\infty} - u^h_{2N} \rvert$	2.664E-2	1.551E-3	3.171E-4	2.371E-4
$\max \lvert p^h_{\infty} - p^h_{N} \rvert$	8.819E-3	6.254E-4	3.313E-5	2.689E-5

Table 6
$\nu = 0.01$, mesh B

N	$N = 0$	$N = 1$	$N = 3$	$N = 5$
$\max \lvert u^h_{1\infty} - u^h_{1N} \rvert$	1.371E-2	2.816E-3	7.528E-5	1.194E-4
$\max \lvert u^h_{2\infty} - u^h_{2N} \rvert$	2.578E-2	3.606E-3	1.229E-4	7.896E-5
$\max \lvert p^h_{\infty} - p^h_{N} \rvert$	6.107E-3	7.554E-4	1.064E-5	1.270E-5

6. Conclusions

A new series of artificial boundary conditions on the outflow boundary is designed for steady two-dimensional incompressible viscous flow in velocity–pressure formulation by imposing the continuity of velocity and normal stress. These boundary conditions are compared to the stress-free boundary condition. Our new boundary conditions are proved to be more accurate. In [3,6,7], the authors show that the stress-free boundary condition is more accurate than Dirichlet boundary condition which is also often used in engineering literatures. Thus, our boundary conditions are also more accurate than Dirichlet boundary condition. Therefore it is time saving, since for a given accuracy it is possible to use a smaller computational domain. We also implement a new artificial boundary condition on inflow boundary. Furthermore, numerical results show that only a few terms in the artificial boundary condition are needed.

Acknowledgements

The author thanks Prof. Houde Han for many helpful discussions on this subject. This work was supported by the Climbing Program of National Key Project of Foundation of China and Doctoral Program Foundation of Institution of Higher Education of China. Computation was supported by the State Key Lab. of Scientific and Engineering Computing in China.

References

[1] L. Halpern, Artificial boundary conditions for the linear advection diffusion equations, Math. Comput. 46 (1986) 425.
[2] L. Halpern and M. Schatzman, Artificial boundary conditions for incompressible viscous flows, SIAM J. Math. Anal. 20 (1989) 308.
[3] F. Nataf, An open boundary condition for the computation of the steady incompressible Navier-Stokes equations, J. Comput. Phys. 85 (1989) 104.
[4] T. Hagstrom, Asymptotic boundary conditions for dissipative waves: General theory, Math. Comput. 56 (1991) 589.
[5] T. Hagstrom, Conditions at the downstream boundary for simulations of viscous, incompressible flow, SIAM J. Sci. Stat. Comput. 12 (1991) 843.
[6] H. Han, J. Lu and W. Bao, A discrete artificial boundary condition for steady incompressible viscous flows in no-slip channel using a fast iterative method, J. Comput. Phys. 114 (1994) 201.
[7] H. Han and W. Bao, An artificial boundary condition for the incompressible viscous flows using the method of lines, Int. J. Numer. Methods Fluids 22 (1996) 483.
[8] H. Han and W. Bao, An artificial boundary condition for the incompressible viscous flows in a no-slip channel, J. Comput. Math. 13 (1995) 51.
[9] W. Bao, Artificial boundary conditions for incompressible viscous flows and its applications, Ph.D. thesis, Tsinghua University, 1995.
[10] R.A. Adams, Sobolev Spaces, 1975.
[11] H. Han, An economical finite element scheme for Navier–Stokes equations, J. Comput. Math. 2 (1987) 5.